PAPER Special Section of Papers Selected from ITC-CSCC '97

Two Dimensional Equalization Scheme of Orthogonal Coding Multi-Carrier CDMA*

Soichi WATANABE†, Takuro SATO†, Masakazu SENGOKU††, *and* Takeo ABE†, *Members*

SUMMARY This paper describes two dimensional (2D) equalization scheme of orthogonal coding multi-carrier CDMA for reverse link of mobile communication systems. The purpose of the 2D equalization is the reduction of Multiple Access Interference (MAI) which is caused by the random access and the different propagation path from each mobile station. The orthogonal coding multi-carrier CDMA multiplexes all mobile stations' data by Code Division Multiplexing (CDM). The 2D coding scheme spreads a preamble signal at time (in subchannel signals) and frequency (between subchannel signals) domains. The 2D decoding scheme estimates transmission delay time and instantaneous fading frequency from preamble signal for individual mobile stations and compensate the received data using these estimation values to reduce MAI.

key words: *MAI, 2D equalization, orthogonal coding, multi-carrier, CDMA*

1. Introduction

Multi-carrier modulation is suitable for high speed data communication and high efficiency transmission systems and it is also robustness for multi-path propagation and frequency selective fading. Recently some researchers began to study for applying the multi-carrier modulation to personal communication systems using Time Division Multiple Access (TDMA) or Code Division Multiple Access (CDMA) [1]–[4]. The interference occurred in the orthogonal coding multi-carrier CDMA are Inter-Channel Interference (ICI) [5], [6], Inter-Symbol Interference (ISI) [7] and Multiple Access Interference (MAI) [8], [9]. The ICI is caused by frequency offset and fading. The ISI is caused by multi-path delay. The MAI is caused by the variation of the transmission delay times and the instantaneous fading frequencies from each mobile station. The transmission delay time influences the phase/amplitude distortion between subchannel signals (frequency domain); the instantaneous fading frequency influences the phase/amplitude distortion in subchannel signals (time domain). Since the frequency deviation and the time deviation change independently for each mobile station on reverse link, that the ICI, the ISI and the MAI fluctuate at every moment occasionally under the actual mobile station environment. When the frequency deviation is lower than the spread rate of the multi-carrier CDMA, the influence of the ICI becomes very small. Guard Interval is used for reduction of the ISI. This paper does not discuss the ICI and the ISI. There are a few publications of the equalization scheme of the phase/amplitude distortion of fading and reduction technologies of MAI. J.Rinne proposed channel phase/amplitude estimation method using Least Square Algorithm (LMS) in frequency domain [10], [11]. He adopted pilot tone for the fast estimation in order to keep up with higher fading frequency. The estimation scheme is effective but this scheme was applied only for the single user detection. Z.Xie et al. proposed Joint Detection (JD) algorithm [8] which estimates the phase/amplitude of received signal using a sub-optimum tree-search algorithm with a recursive least-square method. B.Steiner evaluated the MAI cancellation algorithms [9] using pilot tone scheme which is based on JD algorithm for multi-carrier CDMA. He evaluated some different detection algorithms such as orthogonality restoring correlation matched filtering, serial and parallel interference cancellation algorithms as well as JD algorithms. He showed JD algorithm is the best performance in comparison of other schemes. However JD algorithm does not clarify the reduction of MAI for the variation of the delay times and the instantaneous fading frequencies simultaneously under the multiple access environment because JD algorithm is based on only time domain (1 dimensional) analysis. This paper proposes two dimensional (2D) equalization scheme to overcome large deviation of the delay times and the instantaneous fading frequencies simultaneously. The 2D equalization scheme reduces the MAI using the estimated parameters which is obtained by iterative estimation of the 2D coding preamble signal. The iterative estimation exchanges the estimation parameters of the time and frequency domain equalizers alternately. During the data detection, decision data is obtained after the equalization using estimated values of the delay time and the instantaneous fading frequency which is obtained by the preamble signal. The estimated values are updated by Decision Feedback Equalizer (DFE). The 2D equal-

Manuscript received September 30, 1997.
Manuscript revised December 24, 1997.

†The authors are with the Niigata Institute of Technology, Kashiwazaki-shi, 945–1195 Japan.
††The author is with the Faculty of Engineering, Niigata University, Niigata-shi, 950–2181 Japan.

*This paper was presented in part at the IEICE International Technical Conference on Circuits/Systems, Computers and Communications '97, Okinawa, Japan, July 14-16, 1997.

izer has an advantage that the correct estimated parameters are extracted from multiple access signals under the fading environment. Section 2 describes the System Model for the evaluations and the configuration of the 1D Coding Multi-Carrier CDMA. Section 3 describes the configuration of 2D orthogonal coding multi-carrier CDMA, the channel estimation scheme and the equalization scheme using the 2D preamble signal. Section 4 describes simulation and evaluation results.

2. System Model and One Dimensional Coding Multi-Carrier CDMA

2.1 System Model

Figure 1 shows a system model of a mobile communication system. The dashed lines denote forward link and the solid lines denote reverse link. The mobile stations receive signal from the base station through the forward link synchronously. A base station receives signal from all mobile stations through the reverse link asynchronously, because each mobile station transmits a signal at a different transmission timing and the distances are different between each mobile station and the base station. Phase/amplitude distortions due to fading are also different for each reverse link. MAI is caused by the difference of the transmission delay time and the phase/amplitude distortions. The MAI of the reverse link becomes larger than that of the for ward link because of the asynchronous detection timing and the variations of phase/amplitude due to fading characteristics.

2.2 One Dimensional Coding/Decoding Scheme

Figure 2 (a) shows a configuration of the transmitter of the one dimensional (1D) multi-carrier CDMA. The preamble signal is all "one" and it is spread by Walsh code $\mathbf{W}_m$ of which rate is Lr, where L is the length of the Walsh code. The preamble and data are switched to enter Serial/Parallel (S/P) converter with constant interval. The chip rate of each subchannel is r/L. The subchannel signals are converted to baseband signal through Inverse Discrete Fourier Transformer (IDFT) frame by frame. The frame of the 1D coding scheme is defined as the number of the subchannels ($= L^2$). The transmitter transmits the frame signal though Radio Frequency (RF) modulation. Figure 2 (b) shows a configuration of the receiver. The received signal is converted to subchannel signal through Discrete Fourier Transformer (DFT). The subchannel signal pass through Parallel/Serial (P/S) conversion. The serial signal correlated by Walsh code $\mathbf{W}_m$. The serial signal is compensated by the phase of the propagation path which is obtained by the preamble signals at a phase estimator. Figure 2 (c) shows a frequency response of the subchannel signal of the 1D coding multi-carrier CDMA. The frequency separations between each subchannel are r/L.

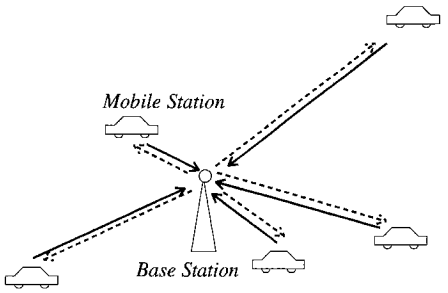

Fig. 1 System model.

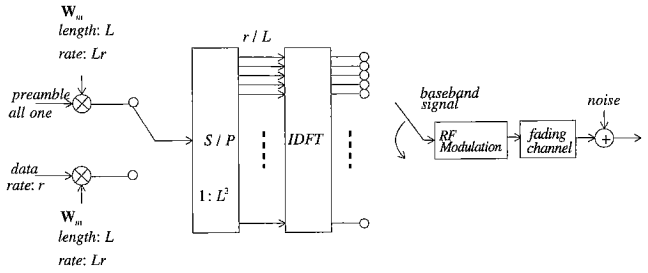

(a) One dimensional coding multi-carrier CDMA.

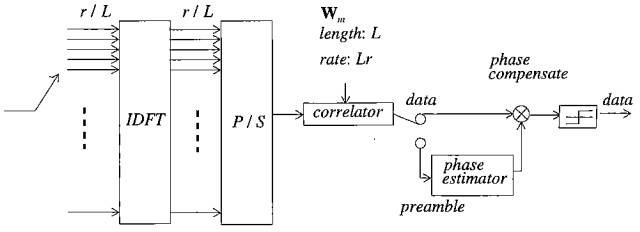

(b) One dimensional decoding.

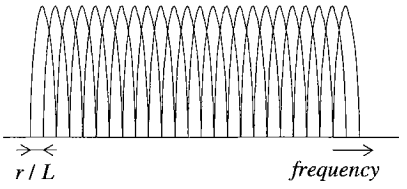

(c) Frequency spectrum of one dimensional coding multi-carrier CDMA.

Fig. 2 One dimensional coding scheme.

It is difficult for the 1D coding scheme to obtain a sufficient BER performance because frequency offset and fading frequency cause large ICI. In this paper, the performance evaluation is based on the baseband model, because the effects of the fading variation, the delay time and AWGN can be directly evaluated by the baseband analysis.

3. Two Dimensional Orthogonal Coding Multi-Carrier CDMA

3.1 Two Dimensional Coding Scheme

Figure 3 (a) shows a configuration of the transmitter of

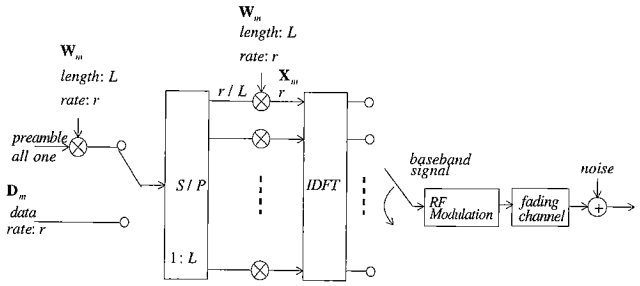

(a) Two dimensional orthogonal coding multi-carrier CDMA.

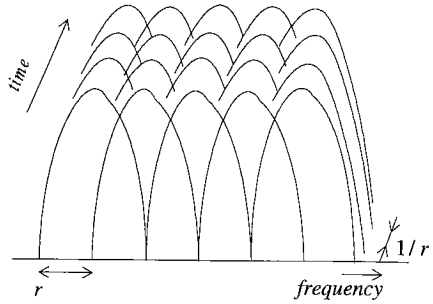

(b) Frequency spectrum of two dimensional orthogonal coding multi-carrier CDMA.

Fig. 3 Two dimensional coding scheme.

two dimensional (2D) orthogonal coding multi-carrier CDMA. The preamble signal is spread by the 2D modulation and the data signal is spread by the 1D modulation. The preamble signal is all "one" and its spreading code is Walsh code $\mathbf{W}_m$ of which rate is r and the length of the Walsh code is L. The spread preamble signal is converted to subchannel signals through S/P. The rate of each subchannel is r/L. Each subchannel signal is spread by Walsh code $\mathbf{W}_m$.

$$\mathbf{X}_m = \mathbf{W}_m \mathbf{D}_m \tag{1}$$

where

$$\mathbf{W}_m = \begin{bmatrix} w_{m,0} \\ \vdots \\ w_{m,i} \\ \vdots \\ w_{m,L-1} \end{bmatrix}$$

$$\mathbf{D}_m = \begin{cases} preamble \\ [w_{m,0} \cdots w_{m,i} \cdots w_{m,L-1}] \\ data \\ [d_{m,0} \cdots d_{m,i} \cdots d_{m,L-1}] \end{cases}$$

Where $w_{m,i}$ is i-th element of Walsh code $\mathbf{W}_m$ and m-th mobile station $d_{m,j}$ is a i-th element of data $\mathbf{D}_m$. The data signal $\mathbf{D}_m = [d_{m,0} \cdots d_{m,1} \cdots d_{m,L-1}]$ of which the data rate is r is converted to subchannel signals through S/P. The spread method of the data on subchannel is same as the spread method of the preamble. The frame of the 2D orthogonal coding scheme is defined as the size of the matrix $\mathbf{X}_m$ $(= L^2)$. The subchannel signals are converted to baseband signal through IDFT and transmitted to air though Radio Frequency (RF) modulation. Figure 3 (b) shows a frequency spectrum of the 2D orthogonal coding multi-carrier CDMA. The frequency separations between each subchannel are r.

3.2 Two Dimensional Decoding

3.2.1 Configuration of Two Dimensional Decoding

In this section, following parameters are defined for analysis equation:

- ε_m is the instantaneous fading frequency of m-th mobile station which is normalized by the chip rate r.
- τ_m is the delay time of m-th mobile station which is normalized by the chip duration T_c.
- a_m is the a reference value of the amplitude of m-th mobile station in a frame, which shows the value at 0-th chip of 0-th subchannel.
- ϕ_m is the reference value of the phase of m-th mobile station in a frame, which shows the value at 0-th chip of 0-th subchannel.
- $\hat{a}_{m,D}$ and $\hat{\phi}_{m,D}$ are the estimated values of a_m and ϕ_m which are obtained by time domain channel estimation.
- $\hat{a}_{m,W}$ and $\hat{\phi}_{m,W}$ are the estimated values of a_m and ϕ_m which are obtained by frequency domain channel estimation.

Figure 4 (a) shows a configuration of the 2D equalizer of the orthogonal coding multi-carrier CDMA. 2D equalizer reduces MAI [Refer to Appendix] using the estimated values obtained by the time and the frequency domain channel estimators. The base station receives incoming signals from all mobile stations simultaneously. The subchannel signals through DFT are correlated by the inverse of the Walsh code matrix $\mathbf{W}^{-1}$ which is compensated by the estimated instantaneous fading frequencies of each mobile station. The estimated instantaneous fading frequencies are obtained by the frequency domain channel estimator. Figure 4 (b) shows the configuration of the phase compensator. The correlate signal is compensated by the estimated values of the delay time $\hat{\tau}_m$ and the reference amplitude/phase $\hat{a}_m e^{j2\pi\hat{\phi}_m}$. The compensated signal feeds to the P/S converter. The decision data $\bar{\mathbf{D}}_m$ is obtained by the decision stage. The decision data is used for Decision Feedback Equalization (DFE) which is shown in Sect. 3.2.5. The decision data feedback to the time and

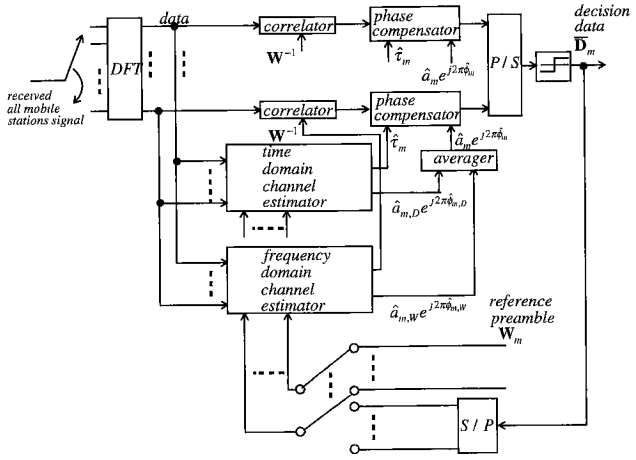

(a) Two dimensional equalizer configuration of orthogonal coding multi-carrier CDMA.

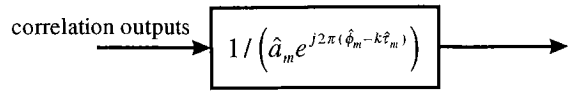

(b) Configuration of phase estimator.

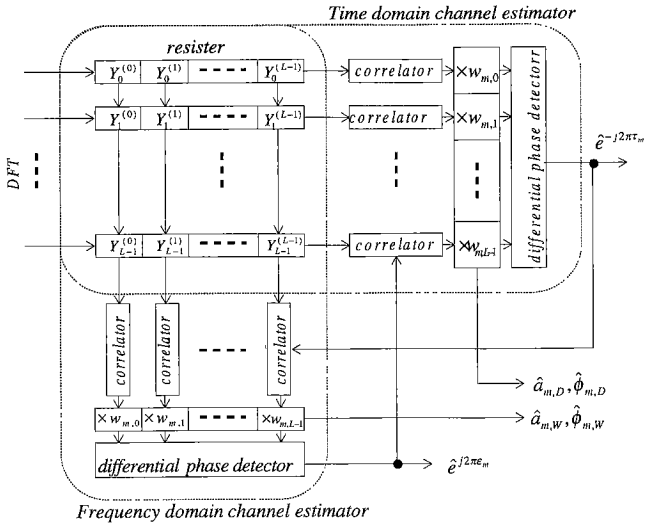

(c) Configuration of time and frequency domain channel estimator.

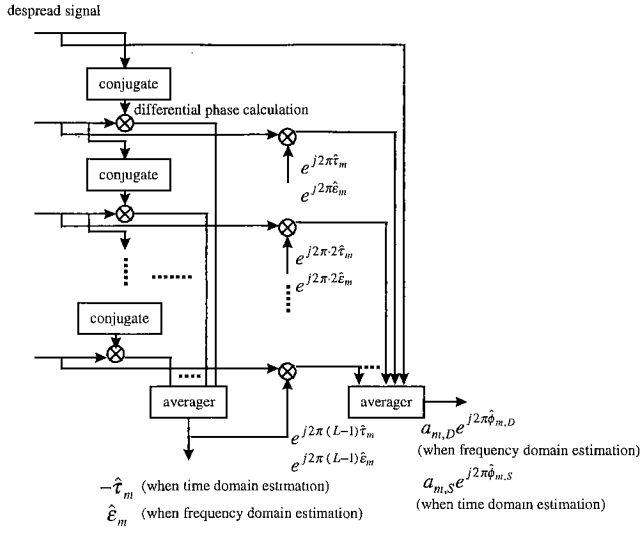

(d) Differential phase detector.

Fig. 4 Two dimensional equalizer.

frequency domain channel estimators in order to estimate the delay times and instantaneous fading frequencies for the next frame. In Fig. 4 (c), the output signals from DFT are stored in two dimensional register frame by frame $L \times L = L^2$. The received frame is influenced by the delay time τ_m and the instantaneous fading frequency ε_m. The received signal from all mobile station is expressed by the product of three matrices.

$$\mathbf{Y} = \mathbf{WAD} + \mathbf{N} \tag{2}$$

where $\mathbf{W}$ is the spread Walsh code matrix, $\mathbf{D}$ is the preamble signal matrix, $\mathbf{A}$ is an amplitude/phase matrix of fading and $\mathbf{N}$ is a additive white Gaussian noise (AWGN) with zero mean and two sided power spectrum density $N_0/2$. The despread Walsh code matrix $\mathbf{W}$ is shown as follows:

$$\mathbf{W} = \begin{bmatrix} w_{0,0} & \cdots & w_{m,0} & \cdots & w_{L-1,0} \\ \vdots & \ddots & & & \vdots \\ w_{0,n} \cdot e^{j2\pi n\varepsilon_0} & & w_{m,n} \cdot e^{j2\pi n\varepsilon_m} & & w_{L-1,n} \cdot e^{j2\pi n\varepsilon_{L-1}} \\ \vdots & & & \ddots & \vdots \\ w_{0,L-1} \cdot e^{j2\pi(L-1)\varepsilon_0} & \cdots & w_{m,L-1} \cdot e^{j2\pi(L-1)\varepsilon_m} & \cdots & w_{L-1,L-1} \cdot e^{j2\pi(L-1)\varepsilon_{L-1}} \end{bmatrix} \tag{3}$$

where the columns and the rows of $\mathbf{W}$ denote the mobile station number m $(= 0, 1, \ldots, L-1)$ and the chip number n $(= 0, 1, \ldots, L-1)$, respectively. $w_{m,n}$ denotes the n-th element of the Walsh code which is assigned for m-th mobile station. ε_m is the instantaneous fading frequency of m-th mobile station. The received signal

matrix $\mathbf{D}$ is shown as follows:

$$\mathbf{D} = \begin{cases} \text{preamble} \\ \begin{bmatrix} w_{0,0} & \cdots & w_{0,k}\cdot e^{-j2\pi k\tau_0} & \cdots & w_{0,L-1}\cdot e^{-j2\pi(L-1)\tau_0} \\ \vdots & \ddots & & & \vdots \\ w_{m,0} & & w_{m,k}\cdot e^{-j2\pi k\tau_1} & & w_{m,L-1}\cdot e^{-j2\pi(L-1)\tau_1} \\ \vdots & & & \ddots & \vdots \\ w_{L-1,0} & \cdots & w_{L-1,k}\cdot e^{-j2\pi k\tau_{L-1}} & \cdots & w_{L-1,(L-1)}\cdot e^{-j2\pi(L-1)\tau_{L-1}} \end{bmatrix} \\ \text{data} \\ \begin{bmatrix} d_{0,0} & \cdots & d_{0,k}\cdot e^{-j2\pi k\tau_0} & \cdots & d_{0,L-1}\cdot e^{-j2\pi(L-1)\tau_0} \\ \vdots & \ddots & & & \vdots \\ d_{m,0} & & d_{m,k}\cdot e^{-j2\pi k\tau_1} & & d_{m,L-1}\cdot e^{-j2\pi(L-1)\tau_1} \\ \vdots & & & \ddots & \vdots \\ d_{L-1,0} & \cdots & d_{L-1,k}\cdot e^{-j2\pi k\tau_{L-1}} & \cdots & d_{L-1,(L-1)}\cdot e^{-j2\pi(L-1)\tau_{L-1}} \end{bmatrix} \end{cases} \tag{4}$$

where the columns and the rows of $\mathbf{D}$ denote the subchannel number k $(= 0, 1, \ldots, L-1)$ and the mobile station number n $(= 0, 1, \ldots, L-1)$, respectively. $w_{m,k}$ and $d_{m,k}$ denote the preamble signal and the data signal of k-th subchannel of m-th mobile station. τ_m is the delay time of m-th mobile station. The matrix $\mathbf{A}$ is a diagonal matrix whose diagonal element denotes the phase/amplitude of each mobile station.

$$\mathbf{A} = \begin{bmatrix} a_0 e^{j2\pi\phi_0} & & & 0 \\ & \ddots & & \\ & & a_m e^{j2\pi\phi_m} & \\ & & & \ddots \\ 0 & & & a_{L-1} e^{j2\pi\phi_{L-1}} \end{bmatrix} \tag{5}$$

where a_m and ϕ_m denote the amplitude and phase of m-th mobile station.

3.2.2 Time Domain Channel Estimator

The time domain channel estimator estimates the delay time $\hat{\tau}_m$ and the amplitude/phase $\hat{a}_{m,D}e^{j2\pi\hat{\phi}_{m,D}}$ of receiving frame. The output of the correlators $\hat{\mathbf{D}}$ is obtained by $\mathbf{W}^{-1}\mathbf{Y}$. It is despreaded by the reference preamble signal $\mathbf{D}_m = [w_{m,0} \cdots w_{m,k} \cdots w_{m,L-1}]$. The differential phase detector, which is shown in Fig. 4 (d), calculates the estimation value of the delay time $\hat{\tau}_m$. It is shown as follows:

$$\hat{\tau}_m = \frac{-1}{2\pi(L-1)} \sum_{k=1}^{L-1} \arg\left(w_{m,k-1} w_{m,k} \hat{D}^*_{m,k-1} \hat{D}_{m,k}\right) \tag{6}$$

where "$*$" denotes a complex conjugate and the subscript of m and k are row and column indices of matrix $\hat{\mathbf{D}}$. From the estimated value $\hat{\tau}_m$, the reference phase/amplitude of each mobile station is calculated as,

$$\hat{a}_{m,D} e^{j2\pi\hat{\phi}_{m,D}} = \frac{1}{L} \sum_{k=0}^{L-1} w_{m,k} \hat{D}_{m,k} e^{j2\pi\hat{\tau}_m k} \tag{7}$$

The average square error of the delay time estimation $\sigma_{\hat{\tau}_m}$ is defined as follows:

$$\sigma_{\hat{\tau}_m} = \frac{1}{L-1} \cdot \sum_{k=1}^{L-1} \left[\frac{-1}{2\pi} \arg\left(w_{m,k-1} w_{m,k} \hat{D}^*_{m,k-1} \hat{D}_{m,k}\right) - \hat{\tau}_m\right]^2 \tag{8}$$

3.2.3 Frequency Domain Channel Estimator

The frequency domain channel estimator estimates the instantaneous fading frequency $\hat{\varepsilon}_m$ and the phase/amplitude $\hat{a}_{m,S}e^{j2\pi\hat{\phi}_{m,S}}$ of receiving frame. The output of the correlators $\hat{S}$ is obtained by $\mathbf{Y}\mathbf{D}^{-1}$. It is despreaded by the Walsh code $\mathbf{W}_m$. The differential phase detector shown in Fig. 4 calculates the estimation value of the instantaneous fading frequency $\hat{\varepsilon}_m$.

$$\hat{\varepsilon}_m = \frac{1}{2\pi(L-1)} \sum_{n=1}^{L-1} \arg\left(w_{m,n-1} w_{m,n} \hat{W}^*_{n-1,m} \hat{W}_{n,m}\right) \tag{9}$$

where the subscript n and m are the row and the column indices of matrix $\hat{W}$. From the estimated value $\hat{\varepsilon}_m$, the reference phase/amplitude of each mobile station is calculated as,

$$\hat{a}_{m,W} e^{j2\pi\hat{\phi}_{m,W}} = \frac{1}{L} \sum_{n=0}^{L-1} w_{m,n} \hat{W}_{n,m} e^{-j2\pi\hat{\varepsilon}_m n} \tag{10}$$

The average square error of the instantaneous fading frequency estimation $\sigma_{\hat{\varepsilon}_m}$ is defined as follows:

$$\sigma_{\hat{\varepsilon}_m} = \frac{1}{L-1} \cdot \sum_{n=1}^{L-1} \left[\frac{1}{2\pi} \arg\left(w_{m,n-1} w_{m,n} \hat{W}^*_{n-1,m} \hat{W}_{n,m}\right) - \hat{\varepsilon}_m\right]^2 \tag{11}$$

3.2.4 Iteration Process

Figure 5 shows the iteration process of the 2D estimation. The delay time $\hat{\tau}_m$, the instantaneous fading frequency $\hat{\varepsilon}_m$ and the phase/amplitude $\hat{a}_m e^{j2\pi\hat{\phi}_m} =$

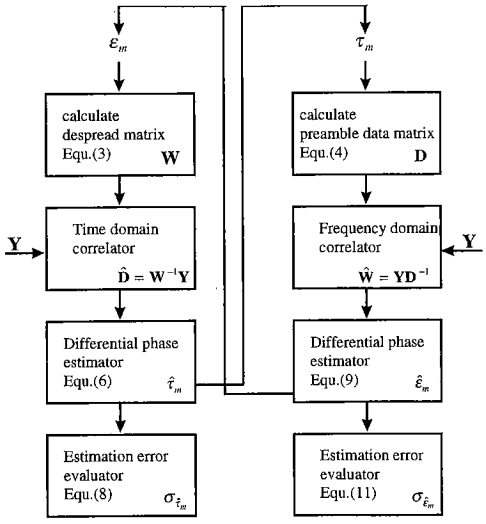

Fig. 5 Estimation process.

$\left(\hat{a}_{m,D}e^{j2\pi\hat{\phi}_{m,D}} + \hat{a}_{m,S}e^{j2\pi\hat{\phi}_{m,W}}\right)/2$ are calculated by the iteration process. The estimates of ε_m and τ_m in previous frame are used as initial estimates of current frame. The left side of Fig. 5 shows the estimation process of the delay time $\hat{\tau}_m$ from the correlation output matrix $\hat{\mathbf{D}}$. The initial values of ε_m is used to calculate the time domain correlation matrix $\mathbf{W}$ in Eq. (3). The time domain correlation output matrix is $\hat{\mathbf{D}} = \mathbf{W}^{-1}\mathbf{Y}$. The estimated delay time $\hat{\tau}_m$ is calculated from Eq. (6). The right side of Fig. 6 shows the estimation process of the instantaneous fading frequency $\hat{\varepsilon}_m$ from the correlation output matrix $\hat{\mathbf{W}}$. The initial value of τ_m is used to calculate the frequency domain correlation matrix $\mathbf{D}$ in Eq. (4). The frequency domain correlation matrix is $\hat{\mathbf{W}} = \mathbf{Y}\mathbf{D}^{-1}$. The estimated value of the instantaneous fading frequency $\hat{\varepsilon}_m$ is calculated from Eq. (9). The estimated values of $\hat{\tau}_m$ and $\hat{\varepsilon}_m$ are exchanged between the time and the frequency domain channel estimators. The iterations are continued until $\sigma_{\hat{\tau}_m}$ and $\sigma_{\hat{\varepsilon}_m}$ becomes lower than the threshold value. After the iteration process, the estimated values of the reference phase/amplitude of each mobile station $\hat{a}_m e^{j2\pi\hat{\phi}_m}$ are obtained by Eqs. (7) and (10).

3.2.5 Decision Feedback Equalizer (DFE)

The Decision Feedback Equalization (DFE) is shown in Fig. 4. During the data detection, the decision data $\bar{\mathbf{D}}_m$ is fedback to the time and the frequency domain channel estimators. The estimation process is same as the preamble detection process. The received data is expressed by Eq. (2). m-th row vectors of the matrix $\mathbf{D}$ in Eq. (4) is replaced by the decision data of m-th mobile station $\bar{\mathbf{D}}_m$. The estimated values of the delay time $\hat{\tau}_m$ and the instantaneous fading frequency $\hat{\varepsilon}_m$ are obtained by Eqs. (6) and (9), respectively. The estimated values are used for the time and the frequency domain channel estimation of the next frame. The estimation values of the phase/amplitude of the next frame is predicted by $\hat{a}_m e^{j2\pi(\hat{\phi}_m - L\hat{\varepsilon}_m)}$.

Table 1 Design parameters.

	1D coding	2D coding
Length of the orthogonal code: L	16	16
Number of subchannel	256	16
Number of mobile station	16	16
Chip duration: T_c	500 μsec	31.25 μsec
Separation of each subchannel	2 kHz	32 kHz
Frame length	500 μsec	500 μsec
Preamble insertion rate	1/4, 1/8	1/4, 1/8

Table 2 Radio channel conditions.

Parameter	Numerical values
Delay time deviation	0.8, 1.6, 3.2 μsec
Fading frequency	50, 100, 150 Hz

4. Simulation and Evaluation

In previous sections, we clarified the estimation algorithm of the delay times and the instantaneous fading frequencies using 2D channel estimatior. In this section, we simulate and evaluate the convergence properties and the bit error rate (BER) characteristics of the 2D orthogonal coding multi-carrier CDMA. Table 1 shows the design parameters of the 2D orthogonal coding multi-carrier CDMA. The radio channel conditions are shown in Table 2. In the simulation, the delay time of each mobile station is assumed to be time invariant because the variation of the delay times due to moving velocities of each mobile station is lower than the variation of the instantaneous fading frequencies due to fading of each mobile station. The transmission channels are modeled as Jakes Rayleigh fading [13] whose distributions of phase and amplitude are uniform and Raylegh distribution, respectively. The estimation process is achieved by the iteration process shown in Fig. 5. The iteration process of the 2D equalization is evaluated by the computer simulation. Figures 6 and 7 show the simulation results of estimation error $\sigma_{\hat{\tau}_m} + \sigma_{\hat{\varepsilon}_m}$ versus iteration steps under 100 Hz and 150 Hz of fading frequencies, respectively. The delay time of each mobile station τ_m and the instantaneous fading frequency ε_m are obtained according to the iteration process. When the iteration process is optimized, the estimation error becomes minimum. When the iteration process fall in the local minimum, the difference between $\hat{a}_{m,D}e^{j2\pi\hat{\phi}_{m,D}}$ and $\hat{a}_{m,W}e^{j2\pi\hat{\phi}_{m,W}}$ are large. In the evaluations of the BER characteristics, the iteration process is continued until the error improvement of the I-th iteration $\Delta\sigma(I)$ becomes 1/10 of the first error improvement $\Delta\sigma(0)$. The transmission channel conditions are E_b/N_0 (10 dB and 20 dB) and the

distribution of the delay time τ_m is Gaussian of which deviations are (0.8 and 3.2 μs). As the results of the simulation, Figs. 6 and 7 show that the estimation error decreases in accordance with the iteration steps. At the environment of large AWGN ($E_b/N_0 = 10$ dB), fast fading frequency ($f_d = 150$ Hz) and large delay time deviation (3.2 μs), the estimation errors are large ($\sigma = 10^{-2}$ to 10^{-3} order). When $E_b/N_0 = 10$ dB, $f_d = 100$ Hz and 0.8 μs of delay time deviation, estimation error becomes 10^{-4} order until five iteration steps.

Figure 8 shows the simulation results of the fault rates of the iteration estimation versus E_b/N_0. The simulation parameters are 100/150 Hz of fading frequencies and 0.8/3.2 μs of the delay time deviations. The maximum number of the iterations is five. The simulation results show that the fault rate is under 0.1 at the con-

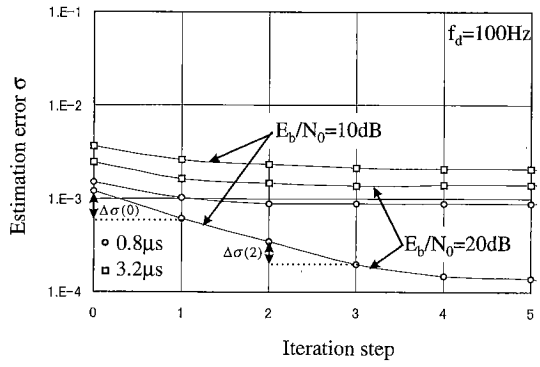

Fig. 6 Simulation results of estimation errors versus iteration steps under 100 Hz of fading frequency.

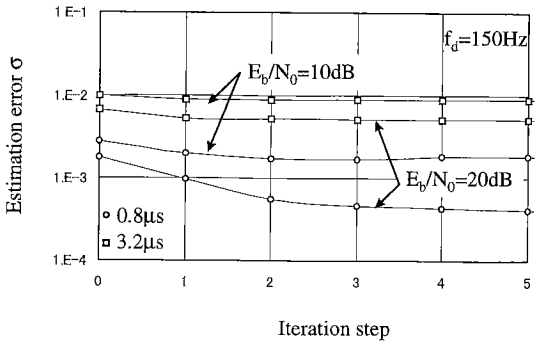

Fig. 7 Simulation results of estimation errors versus iteration steps under 150 Hz of fading frequency.

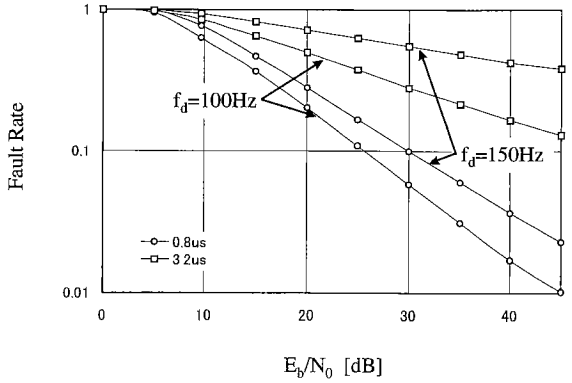

Fig. 8 Fault rates of iteration estimation versus E_b/N_0.

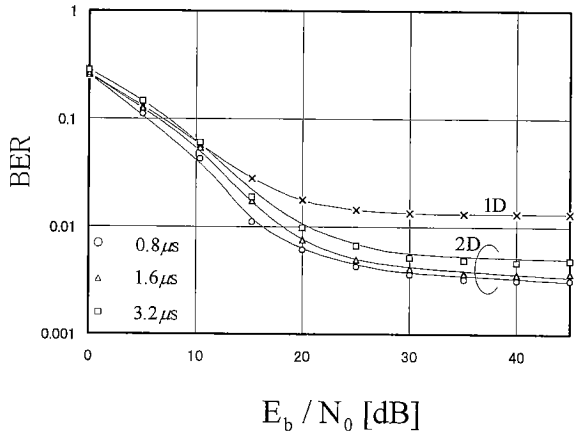

(a) $f_d = 50$ Hz.

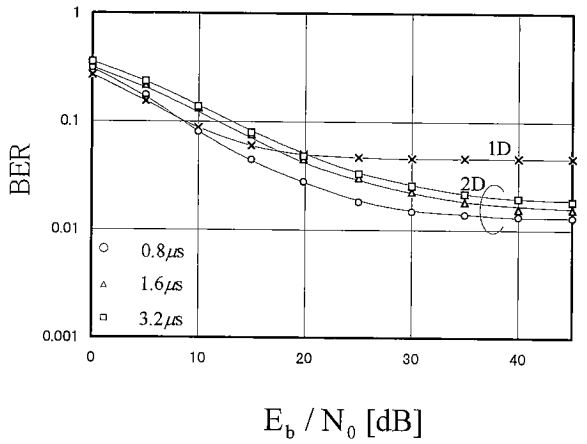

(b) $f_d = 100$ Hz.

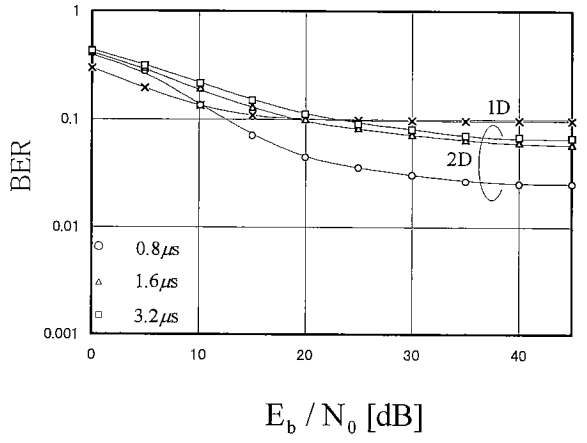

(c) $f_d = 150$ Hz.

Fig. 9 Simulation results of the orthogonal coding multi-carrier CDMA with 1/4 preamble insertion.

dition of 30 dB of E_b/N_0, and 0.8 and 3.2 μs of delay time deviations. Figures 9 and 10 show the simulation results of the BER characteristics of the 2D orthogonal coding multi-carrier CDMA. The BER performance of the 1D coding scheme is also simulated for the comparison with the 2D orthogonal coding scheme. The 1D coding scheme is simulated according to Figs. 2 (a) and (b). The BER characteristics of the 1D coding scheme are same for all examined delay times because the correlation bandwidth is $1/L$ of the 2D coding scheme. In Figs. 9 and 10, when the E_b/N_0 is 20 dB, BER performance of the 2D coding scheme is better than that of the 1D coding scheme because the 2D channel estimator can use the improved estimation values of delay time and instantaneous fading frequency in every frame by DFE. The fault rate which is represented in Fig. 8, is large at 10 dB of E_b/N_0 and the BER performance of the 2D coding scheme is almost same as the 1D coding scheme. Because the new estimation parameters are discarded and the old estimation parameters are used for the 2D equalization. In comparison of the preamble insertion interval of 1/4 in Figs. 9 (a), (b) and (c) and 1/8 in Figs. 10 (a), (b) and (c), the degradation of the BER performances are small in comparison of the 1D coding scheme. Because the 2D coding scheme adopts the decision feedback equalization (DFE) for the data detection. In actual radio channel environments, the variation of the delay time of each mobile station due to moving velocities are small in comparison of the variation of the instantaneous fading frequency. In Figs. 9 and 10, the deviation of the delay times has a little effect for the BER performance compare to that of the fading frequency, since the old estimated value of the delay time $\hat{\tau}_m$ can apply for the equalization of the current frame.

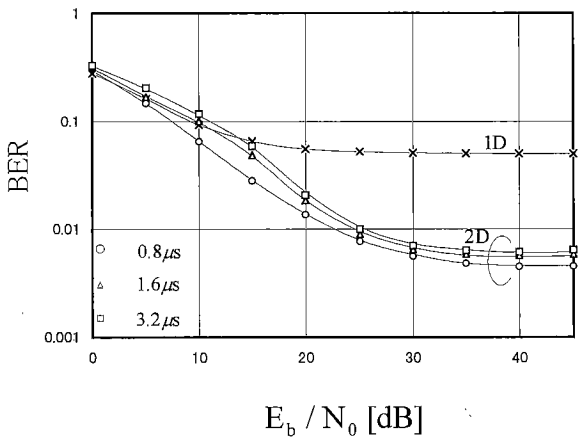

(a) $f_d = 50$ Hz.

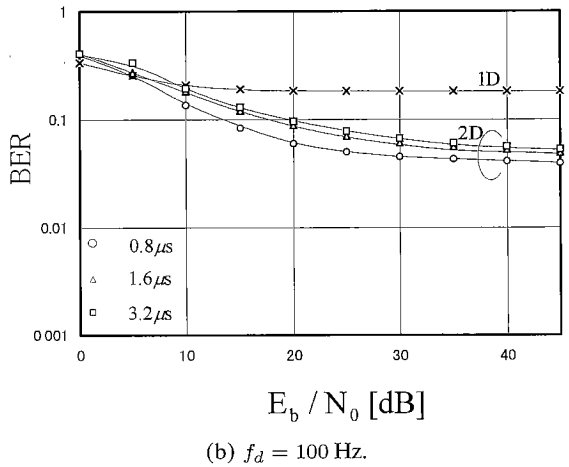

(b) $f_d = 100$ Hz.

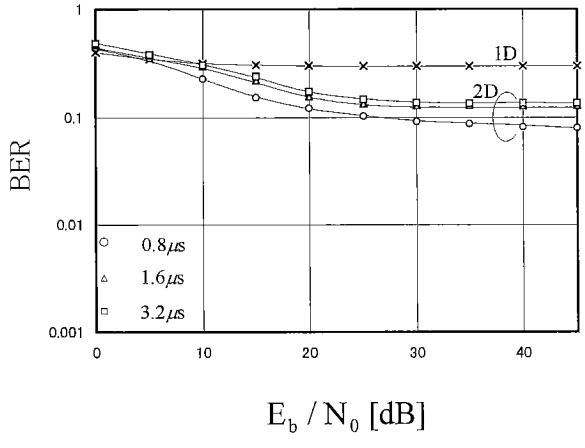

(c) $f_d = 150$ Hz.

Fig. 10 Simulation results of the orthogonal coding multi-carrier CDMA with 1/8 preamble insertion.

5. Conclusion

In this paper, we analyzed the performance of the 2D equalization scheme of the orthogonal coding multi-carrier CDMA for reverse link under fading environment. The 2D equalization scheme reduces the MAI which is caused by the variation of the transmission delay times between each mobile station and the base station and the variation of the instantaneous fading frequencies. The 2D equalization consists of the frequency domain equalizer and the time domain equalizer. The delay times are obtained by the time domain channel estimator and the instantaneous fading frequencies are obtained by the frequency domain channel estimator individually. They exchange estimation parameters between the time and the frequency domain channel estimators to reduce the MAI. This paper also evaluates the BER characteristics of the 1D equalization scheme of the multi-carrier CDMA for a comparison of the 2D equalization scheme. The 2D equalization is superior to reduce the MAI in comparison of the 1D equalization. The 2D equalization scheme can equalize 3.2 μs of deviation of the delay times under 150 Hz of fading frequency. Then it was clarified that the 2D equalization scheme is useful to apply the synchronous detection of the reverse link.

Acknowledgment

Authors would like to thank Dr. Keisuke Nakano, Faculty of Engineering, Niigata University, for his helpful suggestions.

References

[1] M. Alard and R. Lassalle, "Principles of modulation and channel coding for digital broadcasting for mobile receivers," EBU Review Technical, no.224, pp.327–337, Aug. 1987.
[2] T. Muller and R. Grunheid, "Comparison of detection algorithms for OFDM-CDMA in broadband Rayleigh Fading," Proc. IEEE VTC'95, vol.2, pp.835–838, July 1995.
[3] L. Vandendrope, "Multitone spread spectrum multiple access communications system in a multipath rician fading channel," IEEE Trans. Veh. Technol, vol.44, no.2, pp.327–337, May 1995.
[4] Y. Sanada and M. Nakagawa, "A Multiuser Interference Cancellation Technique Utilizing Convolutional Codes and Orthogonal Multicarrier Modulation for Wireless Indoor Communications," IEEE J. Select. Areas Commun., pp.1500–1509, Oct. 1996.
[5] T. Sato, S. Watanabe, and T. Abe, "Synchronization analysis of orthogonal coding multi-carrier CDMA under multipath fading," Proc. ITC-CSCC'96 vol.1, pp.46–49, Seoul Korea 1996.
[6] Y. Zhao and S.G. Haggman, "Sensitivity to doppler shift and carrier frequency errors in OFDM systems," Proc. IEEE VTC'96, pp.1564–1568, May 1996.
[7] S. Watanabe, T. Sato, M. Sengoku, and T. Abe, "Bit error rate evaluation of delay time control scheme for reverse channel on orthogonal coding multi-carrier CDMA," IEICE Trans. Fundamentals, vol.E80-A, no.7, pp.1226–1232, July 1997.
[8] Z. Xie, C.K. Rushforth, R.T. Short, and T.K. Moon, "Joint signal detection and parameter estimation in multiuser communications," IEEE Trans. Commun., vol.41, no.7, pp.1208–1217, Aug. 1993.
[9] B. Steiner, "Uplink performance of a multicarrier-CDMA mobile radio system concept," Proc. IEEE VTC'97, Phoenix, USA, pp.1902–1906, May 1997.
[10] J. Rinne and M. Reforsm, "Equalization of orthogonal frequency division multiplexing signals," Proc. GLOBECOM'94, San Francisco, USA, pp.415–419, Dec. 1994.
[11] J. Rinne, "An equalization method using preliminary decisions for orthogonal frequency division mulitplexing systems in channels with frequency selective fading," Proc. VTC'96, Atlanta, USA, pp.1579–1583, 1996.
[12] S. Watanabe, T. Sato, M. Sengoku, and T. Abe, "Equalization scheme on two dimensional orthogonal coding multicarrier CDMA," Proc. ITC-CSCC'97, Okinawa, Japan, vol.2, pp.1121–1124, 1997.
[13] W.C. Jakes, Jr., "Microwave Mobile Communications," pp.70–76, John Wiley & Sons, NewYork, 1974.

Appendix: Multiple Access Interference (MAI)

The MAI is caused by the phase rotation Δ due to the difference of the transmission delay time and the difference of the instantaneous fading frequency of each mobile station. When the difference of the phase rotation between m-th mobile station and m'-th mobile station

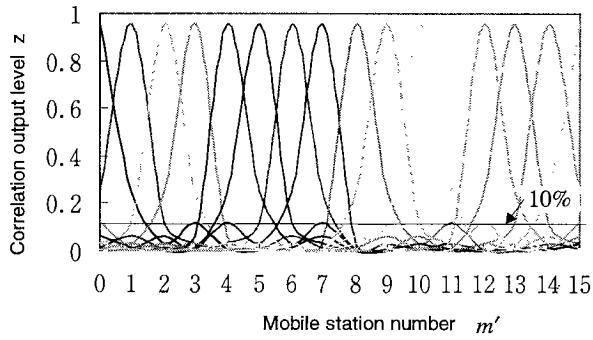

(a) $\Delta = 0.01$ Correlation output level influenced by MAI.

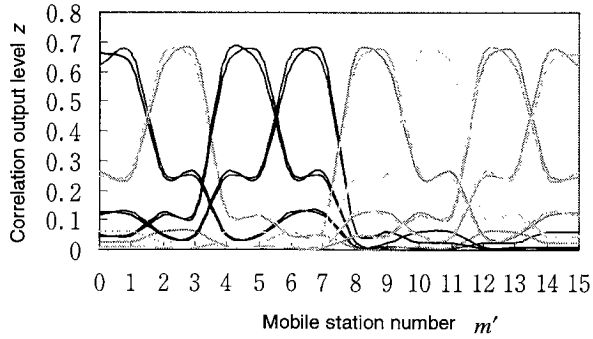

(b) $\Delta = 0.03$ Correlation output level influenced by MAI.

Fig. A·1 Correlation output level influenced by MAI.

is $2\pi\Delta$, the correlation output of the m-th mobile station which is influenced by the m'-th mobile station is shown as follows:

$$z = \sum_{i=0}^{N-1} e^{j2\pi\Delta i} w_{m,i} w_{m',i} \qquad \text{(A·1)}$$

where $w_{m,i}$ is i-th element of Walsh code for m-th mobile station. The correlation output z are MAI when $m \neq m'$ and z is detected signal amplitude when $m = m'$. Figure A·1 shows the level of the correlation outputs influenced by the MAI calculated from Eq. (A·1) for the case of (a) $\Delta = 0.01$ and (b) $\Delta = 0.03$. When $N = 16$, the phase rotation $\Delta = 0.01$ corresponds to 0.32π rad and $\Delta = 0.0315$ corresponds to π rad in one preamble frame. The interference of the MAI are (a) 10% of the detected signal level and (b) almost same as the detected signal level.

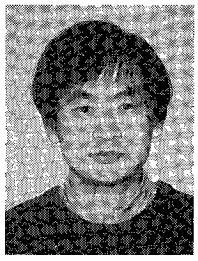

Soichi Watanabe was born in Japan 1969. He received the B.S. (EE) and M.S. (EE) degrees from Niigata University in 1991 and 1993, respectively. He is presently working in Niigata Institute of Technology, Japan. His current research interest is multi-carrier communication systems.

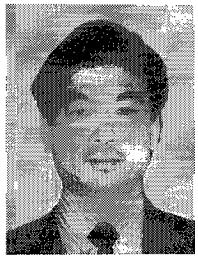

Takuro Sato was born in Niigata prefecture, Japan, On January 16, 1950. He received the B.E. and Ph.D. degrees in electronics engineering from Niigata University, in 1973 and 1994, respectively. He was with Research and Development Laboratories, Oki Electric Industry Co., Ltd., Tokyo, Japan, on PCM transmission equipment, mobile telephone, mobile data transmission, nonlinear system and neural network. He is currently Professor, Department of Information and Electronics Engineering, Niigata Institute of Technology. His current research is in personal communication systems, digital signal processing and automatic control system.

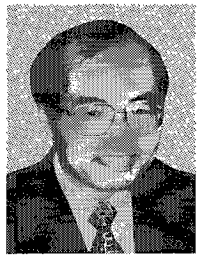

Masakazu Sengoku received the B.E. degree in electrical engineering from Niigata University, Niigata, Japan, 1967 and the M.E. and Ph.D. degrees from Hokkaido University in 1969 and 1972, respectively. In 1972, he joined the staff at Department of Electronic Engineering, Hokkaido University as a Research Associate. In 1978, he was an Associate Professor at Department of Information Engineering, Niigata University, where he is presently a Professor. His research interests include network theory, graph theory, transmission of information and mobile communications. He received the Paper Awards from IEICE in 1992, 1996 and 1997, and IEEE ICNNSP Best Paper Award in 1996. He was 1995 Chairman of IEICE Technical Group on Circuits and Systems (TG-CAS). He is a senior member of IEEE, a member of the Information Processing Society of Japan and Japan Society for Industrial and Applied Mathematics.

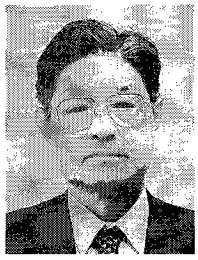

Takeo Abe received the B.E. and Dr. Eng. degrees from Tokyo Institute of Technology in 1949 and 1966, respectively. From 1950 to 1959, he was a Research Scientist at the Electrotechnical Laboratory, Tokyo. From 1962 to 1966 he was an Associate Professor at Tokyo Institute of Technology. From 1966 to 1991 he was a Professor at Niigata University. From 1991 to 1995 he was a Professor at Chiba Institute of Technology. He is now President of Niigata Institute of Technology. He received the Paper Awards from IEICE in 1992 and 1997, and IEEE ICNNSP Best Paper Award in 1996. His interests are in the field of electromagnetic theory, transmission of information and network theory. He is a member of IEEE.